Mass and β decay of the new neutron-rich isotope ^{60}Mn

Eric B. Norman*
Physics Division, Argonne National Laboratory, Argonne, Illinois 60439
and University of Chicago, Chicago, Illinois 60637

Cary N. Davids, Martin J. Murphy,† and Richard C. Pardo‡
Physics Division, Argonne National Laboratory, Argonne, Illinois 60439
(Received 6 March 1978)

The new isotope ^{60}Mn was produced by bombarding ^{48}Ca with ^{18}O ions at $E_{^{18}O} = 50$–70 MeV. The β-decay scheme of ^{60}Mn was determined from γ-ray singles and γ-γ coincidence experiments using large Ge(Li) detectors. The half life of ^{60}Mn was found to be 1.79 ± 0.10 s. A new level with excitation energy 2792 keV was observed in the daughter, ^{60}Fe. The ground-state spin and parity of ^{60}Mn was determined to be 3^+ and its total decay energy Q_β was measured to be 8.51 ± 0.10 MeV. This corresponds to a mass excess of -52.89 ± 0.10 MeV, which is compared with various predictions. The structure of ^{60}Fe as determined from the present work and from previous experiments is compared with a shell-model calculation.

[RADIOACTIVITY ^{60}Mn: measured $T_{1/2}$, E_γ, I_γ, E_β, γ-γ coin, β-γ coin; deduced decay scheme, logft, mass excess, g.s. J^π. ^{60}Fe: deduced levels. Enriched targets, Ge(Li) detectors, plastic scintillator, multiple rabbit.]

I. INTRODUCTION

A program to study the β-decay properties of nuclei far from stability in the $1f$-$2p$ shell has been underway at Argonne National Laboratory for several years. These studies provide information that is useful to both nuclear physics and astrophysics. Spectroscopic information is obtained on the daughter nuclides, and it is usually possible to determine, or at least set limits on, the J^π values of the parent ground states. The measured mass excesses and logft values are useful for testing mass predictions and for establishing β-decay systematics, both of which are needed in nucleosynthesis calculations. Studies of the $T_z = \frac{9}{2}$ nuclei ^{51}Sc (Ref. 1), ^{53}Ti (Ref. 2), ^{57}Cr (Ref. 3), and ^{59}Mn (Ref. 4) have been previously reported. The present study deals with the β-decay of the new neutron-rich isotope ^{60}Mn. A preliminary report on the decay of ^{60}Mn has appeared in Ref. 5.

Until recently, little was known about the structure of the ^{60}Mn decay daughter, ^{60}Fe. The results of recent ^{48}Ca(^{18}O, $\alpha 2n\gamma$)^{60}Fe (Refs. 6 and 7), ^{48}Ca(^{15}N, $2np\gamma$)^{60}Fe (Ref. 7), ^{58}Fe($t, p\gamma$)^{60}Fe (Ref. 7), and ^{58}Fe(t, p)^{60}Fe (Ref. 8) experiments have provided new information on the energies, spins, and parities of states in ^{60}Fe. The last reaction also provided an accurate mass excess for ^{60}Fe of -61.404 ± 0.005 MeV, which was needed to calculate the ^{60}Mn mass excess from the present Q_β measurement.

In the present work, we have measured the γ-ray singles and γ-γ coincident spectra following the β-decay of ^{60}Mn. γ rays have been attributed to the decay of ^{60}Mn by comparisons of their energies with those of previously reported levels in ^{60}Fe and by their coincidence relations with known γ-rays in ^{60}Fe. From these measurements, the half life, ground-state spin, parity, and decay scheme of ^{60}Mn were determined. In addition, a β-γ coincidence experiment was performed to measure the total decay energy Q_β. The resulting mass excess of ^{60}Mn is compared with various predictions. The level structure of ^{60}Fe deduced from the present and previous measurements is compared with a shell-model calculation.

II. EXPERIMENTAL METHOD

The isotope ^{60}Mn was produced by bombarding ^{48}Ca targets with 50–70-MeV ^{18}O ions. The predominant reaction responsible for the production of ^{60}Mn at these energies is most likely ^{48}Ca(^{18}O, αpn)^{60}Mn. All of the data presented in this paper were obtained using a bombarding energy of 56 MeV, because an initial survey indicated that this energy produced the highest yield of ^{60}Mn relative to other contaminant radioactive species. The compound-nucleus evaporation code ALICE[9] predicts a ^{60}Mn production cross section of 80 μb at this bombarding energy. Beam currents of 50–200 nA (electrical) of $^{18}O^{6+}$ ions were supplied by the Argonne National Laboratory tandem ac-

celerator. Each target assembly consisted of a 96.8% enriched ^{48}Ca rolled foil 1.17 mg/cm^2 thick placed on a 0.05 mm tantalum backing which was mounted on a Delrin holder. Approximately 100 μg/cm^2 of gold was flashed over the calcium to inhibit oxidation. The targets were irradiated *in vacuo* and then transferred to a shielded counting area using a multiple-target pneumatic transfer system (multiple rabbit) described in detail by Parks *et al.*[10] This device can hold up to eight targets. After a target is activated, transferred, counted, and returned, a new target is rotated into place. This allows time between bombardment/count cycles which reduces the buildup of unwanted long-lived activities. Control of bombardment, target transfer, and computer gating functions was accomplished by means of a crystal-controlled sequence timer.

Delayed γ rays were measured using one or two 15% efficient Ge(Li) detectors. In order to reduce the number of β particles entering the detectors, Lucite absorbers of 0.65-cm thickness were placed between the sample and the detector(s). A 4.4-cm deep by 7-cm diameter NE102 plastic scintillator coupled to an RCA8575 phototube was used to detect β^- particles in coincidence with decay γ rays. Energy and efficiency calibrations of the γ-ray detectors were performed using standard γ-ray sources.

In the singles measurement, γ spectra were routed into eight 4096-channel time bins, each of 1-s duration. Separate scaling of a pulser, gated by the busy signal from the analog-to-digital converter, provided dead-time information. The overall resolution was typically 2.5 keV (full width at half-maximum) for the 1332-keV line of ^{60}Co.

Coincidence experiments were performed using constant fraction timing techniques with commercially available electronics. In the β-γ coincidence experiment, a pile-up rejector was used with the plastic scintillator. Data for both γ-γ and β-γ coincidence experiments were recorded on magnetic tape for subsequent off-line analysis. Coincident γ ray or β^- spectra were produced from events in one detector by setting windows on γ-ray peaks of interest in the other detector. These spectra were corrected for background-coincident events by subtracting spectra obtained by setting windows on background regions both above and below the peaks of interest.

III. RESULTS

A. Half-life and decay scheme of ^{60}Mn

^{60}Mn was identified by the observation of an 823.6-keV γ ray which decayed with a half life of approximately 2 s. This energy agreed with previous measurements of the energy of the first excited state of ^{60}Fe.[6,7] Other strong γ rays with energies of 492.9 and 1968.8 keV were also observed to decay with half-lives near 2 s.

The half-life of ^{60}Mn was determined by observing the decays of the 823.6- and 1968.8-keV γ rays. After correction for dead time, the composite decay curve for these two γ rays yielded a half-life of 1.79 ± 0.10 s.

More than one hundred γ rays were observed in the singles spectra following the bombardment of ^{48}Ca with 56-MeV ^{18}O. In order to make short-lived activities stand out among such a large number of γ rays, a useful technique is to subtract the sum of the spectra in time bins 5, 6, 7, and 8 from the sum of the spectra in time bins 1, 2, 3, and 4 after correcting for system dead time. The result of this operation is shown in Fig. 1 to illustrate the singles data. The dead-time correction procedure used to produce this spectrum was to make the yields of the 1163.5-keV γ ray from the decay of the 13.9-m ^{62}Co^m equal in all time bins before the appropriate additions and subtractions were performed. This spectrum has also been approximately corrected for detector efficiency by multiplying the contents of each channel by the channel number.

In order to determine the decay scheme of ^{60}Mn, a γ-γ coincidence experiment was performed. Two examples of the coincidence spectra obtained in this experiment are shown in Fig. 2. Four previously unassigned γ rays were identified in the coincidence gates. γ rays with energies of 1290.2, 1475.3, and 2299.3 keV, which had been obscured in the singles spectra by contaminant γ rays of nearly the same energies, appeared in the coincidence data. In addition, a 678.2-keV transition, which had been seen weakly in the singles spectra, appeared in the 1290-keV coincidence gate. A 271.8-keV γ ray was observed in the singles data to decay with a half-life of 1.84 ± 0.23 s, which is approximately equal to that of the ^{60}Mn decay γ rays. This γ ray, however, did not appear in any of the coincidence gates that were set. Furthermore, the intensity of this γ ray relative to ^{60}Mn decay γ rays did not remain constant when the ^{18}O bombarding energy was varied. As a result, this γ ray was not assigned to the decay of ^{60}Mn.

The energies and relative intensities of the γ rays attributed to the decay of ^{60}Mn are summarized in Table I. The γ-ray intensities were normalized with respect to the intensity of the 823.6-keV γ ray and were corrected for coincidence summing. The relative intensity of the 1290.2-keV γ ray had to be determined from the 824-keV coincidence spectrum because of the interference from other γ rays in the singles spectra. For

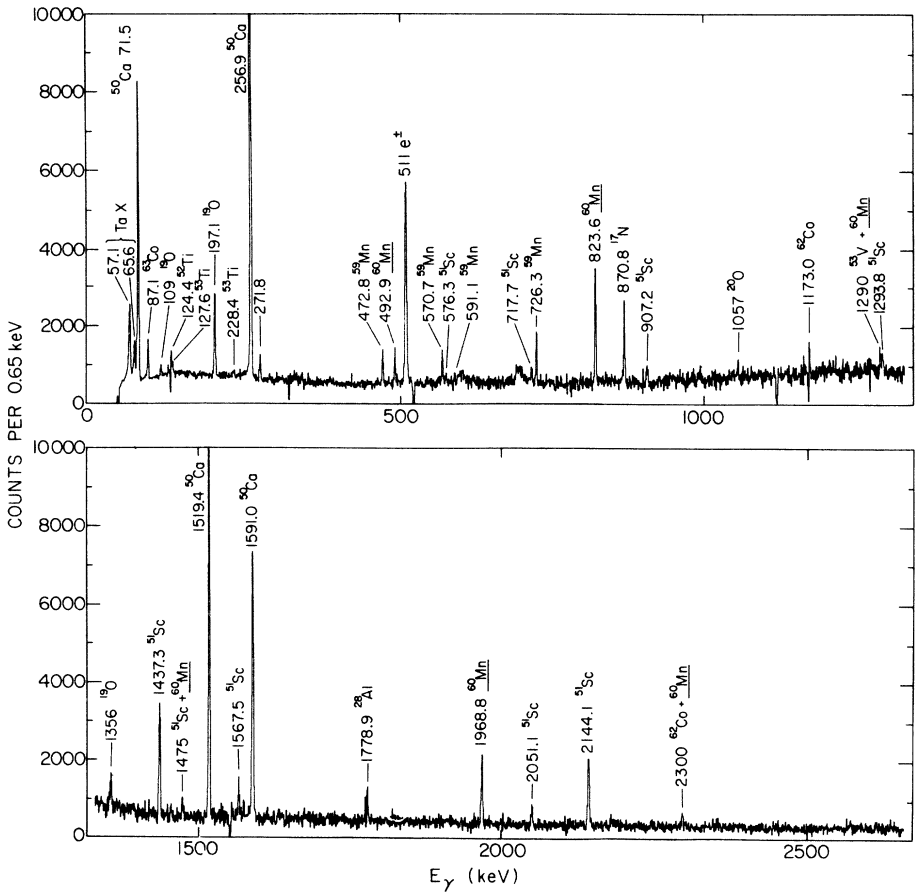

FIG. 1. β-delayed γ-ray singles spectrum observed following the bombardment of ^{48}Ca with 56-MeV ^{18}O. A spectrum obtained during a 4-s period has been subtracted from that obtained in the previous 4 s. The spectrum has been approximately corrected for detector efficiency by multiplying the contents of each channel by the channel number.

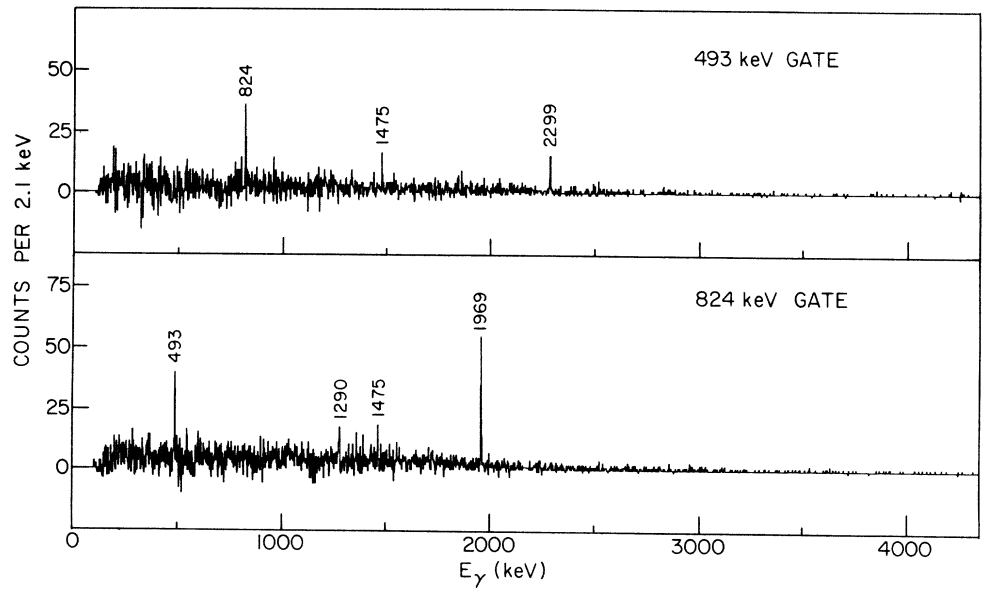

FIG. 2. Backgound-corrected γ spectra observed in coincidence with the 493- and 824-keV γ rays.

TABLE I. Energies and relative intensities of γ rays in ^{60}Fe observed following the β decay of ^{60}Mn.

E_γ (keV)	I_γ (Relative)
492.9 ± 0.3	24.4 ± 1.3
678.2 ± 0.7	3.0 ± 0.7
823.6 ± 0.3	100
1290.2 ± 0.7	13.9 ± 1.3
1475.3 ± 0.7	14.6 ± 1.4
1968.8 ± 0.5	71.1 ± 3.6
2299.3 ± 0.9	17.6 ± 2.0

this transition, it was assumed that the relative detection efficiency was unaffected by the coincidence circuitry. The relative intensities of all the other ^{60}Mn decay γ rays were determined from the singles measurements.

Using the results of the γ-ray singles and γ-γ coincidence experiments, the decay scheme of ^{60}Mn shown in Fig. 3 was constructed. All seven γ rays attributed to the decay of ^{60}Mn have been placed in this scheme. The levels at 823.6, 2114, and 2299 keV were previously observed in in-beam γ ray[6,7] and in charged-particle[8] studies of ^{60}Fe. The 2792.3-keV level was not previously reported. The excitation energies of the 823.6-, 2114-, 2299-, and 2792.3-keV levels have estimated uncertainties of 0.3, 1, 1, and 0.6 keV, respectively.

The β-branching ratios shown in Fig. 3 were calculated from the intensity balance of γ rays for each state in ^{60}Fe. In these calculations, it was assumed that there is no β branch to the ^{60}Fe ground state. Log*ft* values have been determined from the tables of Gove and Martin[11] by using a total decay energy of 8.51 MeV as discussed below.

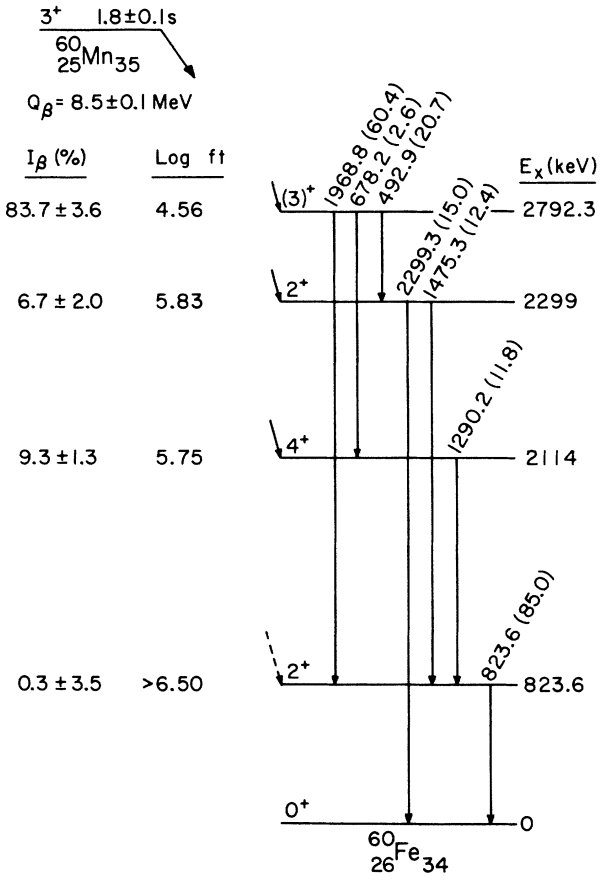

FIG. 3. The decay scheme of ^{60}Mn. Only those ^{60}Fe levels involved in the decay of ^{60}Mn are shown. The γ-ray energies and relative intensities were measured in the present work. The spin and parity assignments are discussed in the text. The numbers enclosed by parentheses are the γ-ray yields per 100 ^{60}Mn decays.

B. Mass of ^{60}Mn

The total β-decay energy of ^{60}Mn was measured in a β-γ coincidence experiment. Data were cyclically accumulated in 4-s counting periods following 3-s irradiations of the targets. Digital gates were set on the 492.9- and 1968.8-keV γ rays and on background regions both above and below these peaks. The background-corrected β spectra coincident with the 492.9- and 1968.8-keV γ rays, respectively, were added together and the resulting spectrum is shown in Fig. 4.

The end-point energy of this β spectrum was determined by using the shape-fitting technique described by Davids *et al.*[12] This method utilizes a least-squares minimization procedure to stretch or compress a standard β spectrum along the energy (horizontal) axis and to normalize the resulting spectrum in order to fit other β spectra. β spectra with well-known end-point energies from the decays of other isotopes produced in the same β-γ experiment are fitted by this method. A similar fit is made to the β spectrum whose end-point energy is to be determined. The stretch factors calculated for the known isotopes are then plotted as a function of end-point energy and a linear least-squares fit is made to the data. The energy calibration provided by this fit, together with the stretch factor determined for the unknown spectrum, is used to calculate the unknown end-point energy.

A major reason for using this technique is that most of the data points in the spectrum may be used in the fitting procedure. A second reason is that experimental problems such as poor detector resolution, losses of β particles from the edges of the detector, backscattering, and energy

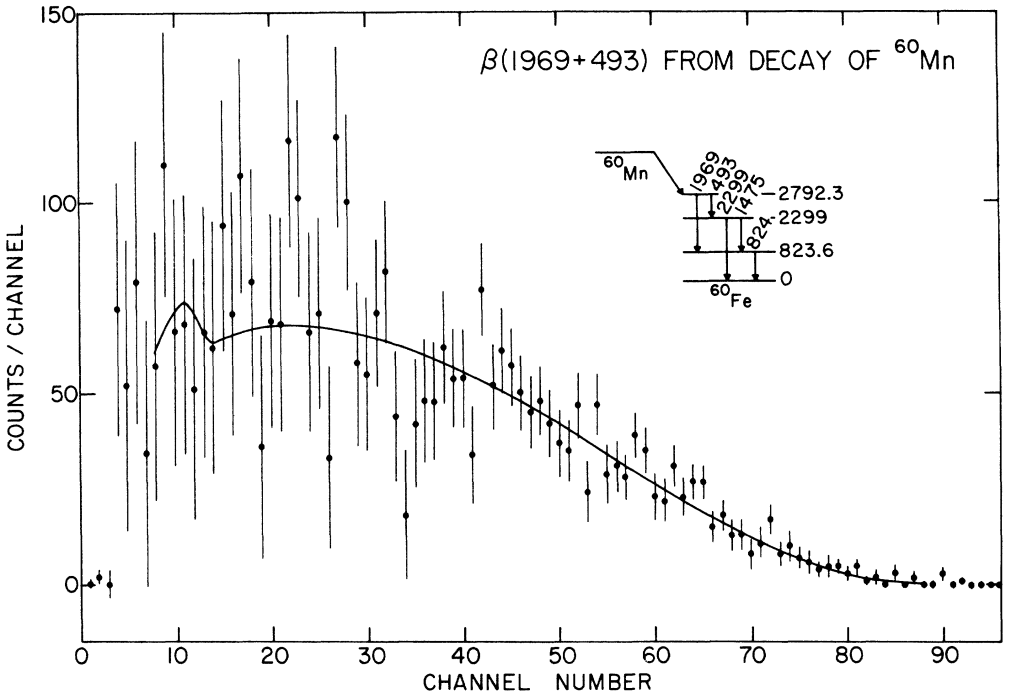

FIG. 4. Background-corrected β spectrum from the decay of ^{60}Mn to the 2792.3-keV state in ^{60}Fe. The smooth curve is a fit made to the data as described in the text. The decay scheme shown in the inset includes only those ^{60}Fe levels and γ rays that are involved in producing this β spectrum.

losses in the material between the source and the detector all affect the observed shapes of β spectra. By using an experimentally obtained β spectrum as a standard, the major influences of these effects are automatically included in the end-point determination.

The standard used in the present measurement was taken from the β spectrum coincident with the 1779-keV γ ray from the decay of ^{28}Al. This isotope was produced by the ^{12}C(^{18}O, pn)^{28}Al reaction on hydrocarbon contaminants which accumulated on the targets. The resulting spectrum shown in Fig. 5 is a pure β^- spectrum with an end-point energy of 2865±2 keV. The smooth curve, drawn through the data by hand, was then used as the standard shape. The accuracy of this hand-drawn fit was checked by fitting the original ^{28}Al data with this standard.

Similar γ-ray-coincident β spectra from the decays of other isotopes were also produced. These spectra were fitted by using the techniques described above. Table II lists the isotopes whose β spectra were fitted, the energies of the coincident γ rays, the known β end-point energies, and the resulting stretch factors. The fitting region and χ_ν^2, the reduced χ^2, of each fit is also

TABLE II. Stretch fit results for nuclei with known β end-point energies.

Nucleus	γ ray (keV)	Region fit (Channel Nos.)	Stretch factor	χ_ν^2	β end point (keV)
^{51}Ti	320	10-38	0.735±0.003	1.62	2146± 4
^{49}Ca	3084	8-36	0.750±0.005	0.93	2184± 7
^{20}O	1057	8-35	0.965±0.045	1.12	2759± 9
^{28}Al	1779	5-48	1.000±0.001	0.70	2865± 2
^{50}Ca	1519+1591	8-50	1.079±0.007	1.49	3120±18
^{19}O	1357	8-50	1.142±0.008	0.95	3265± 4
^{50}Sc	524	9-61	1.298±0.007	1.55	3694±17
^{15}C	4277 (D.E. of 5299)	10-64	1.571±0.012	2.14	4473± 2

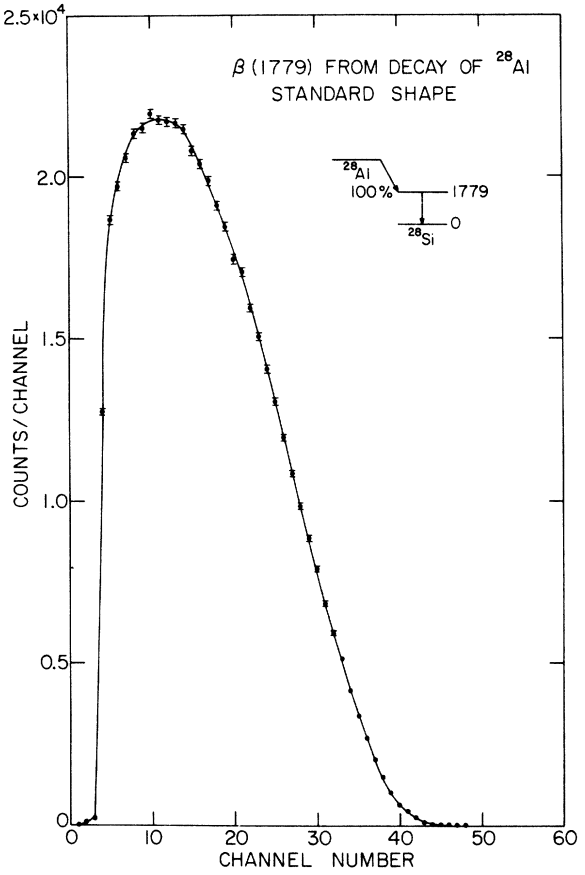

FIG. 5. Background-corrected β spectrum from the decay of ^{28}Al to the 1779-keV state in ^{28}Si. The smooth hand-drawn curve through the data is the "standard shape" described in the text.

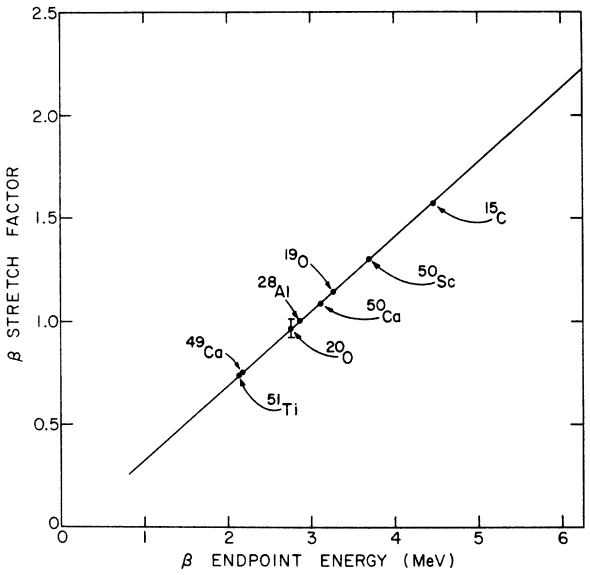

FIG. 6. β end-point energy calibration for the known β spectra obtained in the β-γ coincidence experiment. The straight line is a linear least-squares fit to the data which are listed in Table II.

listed. All of the spectra used in the present analysis are pure β spectra produced by allowed transitions. As described above, a linear least-squares fit was made to a plot of the calculated stretch factors versus end-point energies. The results of this procedure are shown in Fig. 6. This fit was used as the calibration for determining the end-point energy of the β-decay branch of ^{60}Mn to the 2792.3-keV level in ^{60}Fe.

The effects of coincident γ rays and of multiple β feedings can be included in the present method of analysis. The solid curve shown in Fig. 4 is the result of a fit to the data made by assuming the decay scheme shown in the inset. The peak in the curve near channel 11 represents the Compton edge of the coincident 824-keV γ ray. The value of the stretch parameter deduced from this fit to the β spectrum of ^{60}Mn is listed in Table III. Combining this stretch factor with the results of the calibration yields the end-point energy also given in Table III. The total β-decay energy Q_β is obtained by adding the 2792.3-keV excitation energy in ^{60}Fe to this end-point energy, and the result is 8.51 ± 0.10 MeV. Using the value of the mass excess of ^{60}Fe measured by Norman *et al.*,[8] the resulting mass excess of ^{60}Mn is −52.89 ± 0.10 MeV. The quoted uncertainty includes a 50-keV systematic uncertainty for the shape-fitting procedure.

C. Ground-state spin and parity of ^{60}Mn

The spins and parities of the levels at 2114- and 2299-keV excitation energy in ^{60}Fe have been shown by previous workers[7,8] to be 4^+ and 2^+, respectively. The measured log*ft* values of the transitions to these states are both <5.9. Ac-

TABLE III. Stretch fit results for ^{60}Mn.

E_γ (keV)	E_x (keV)	Stretch factor	χ_ν^2	Region fit (Channel Nos.)	Measured β end point (keV)	Q_β (keV)
(493 + 1969)	2792.3	2.03 ± 0.03	0.92	8 − 78	5714 ± 86	8506 ± 86

cording to the rules deduced by Raman and Gove,[13] these β branches thus are allowed transitions. Therefore, in these transitions, J can change by 0 or ± 1 with no change in parity. These considerations uniquely determine the ground-state spin and parity of ^{60}Mn to be 3^+.

D. Spin and parity of the 2792.3-keV level in ^{60}Fe

As was mentioned above, the only level in ^{60}Fe observed in the decay of ^{60}Mn that had not been previously reported is the 2792.3-keV level. The measured logft value of the β branch to this state is 4.56. Thus, according to the rules of Raman and Gove,[13] this transition is definitely allowed. Knowing that the spin and parity of ^{60}Mn is 3^+ then restricts the spin and parity of the 2792.3-keV state to be 2^+, 3^+, or 4^+.

If the spin and parity of this state were 2^+, then it might be expected to decay to the (0^+) level at 1975 keV and/or to the 0^+ ground state. However, neither transition is observed. If the spin and parity were 4^+, then 492.9- and 1968.8-keV transitions would both be $E2$. The estimated $E2$ single-particle rate of the 1968.8-keV transition is more than 1000 times faster than that of the 492.9-keV transition. Thus, in order to explain the observed branching ratios, the 492.9-keV transition would have to be enhanced by a factor of more than 340 relative to the 1968.8-keV transition. Such a large relative enhancement is unlikely. The fact that the 2792.3-keV level was not observed in $(t,p\gamma)$ (Ref. 7) or (t,p) (Ref. 8) studies of ^{60}Fe suggests that this state could have unnatural parity, for it is well known that the (t,p) reaction tends to strongly populate only natural-parity states. The only unnatural-parity state that could be fed by an allowed transition is a 3^+ state. It has been observed that the decay of ^{58}Mn has a 76% branch to a 3^+ state at 2134-keV excitation in ^{58}Fe.[14] Perhaps an analogous situation exists in the decay of ^{60}Mn. As a result of these considerations, we suggest a spin and parity of $(3)^+$ for the 2792.3-keV level in ^{60}Fe, although the 2^+ and 4^+ possibilities are not ruled out.

IV. DISCUSSION

A. Mass of ^{60}Mn

In Table IV, the measured value of the mass excess of ^{60}Mn is compared with various mass predictions. The measured Q_β is also compared with the values predicted by these models. The Q_β values not enclosed by parentheses were calculated using the mass excess of ^{60}Fe measured by Norman *et al.*[8] The Q_β values in parentheses were calculated using the ^{60}Fe mass excess predicted by the various models. These comparisons show that the predictions vary from one another by as much as 1.6 MeV and from the measured value by as much as 0.9 MeV. The updated Garvey-Kelson prediction of Jänecke[15] and the droplet model prediction of Myers[15] show the best agreement with the measured mass excess value.

TABLE IV. Comparison of measured ^{60}Mn mass excess (ME) and Q_β with predictions.

Source	ME (MeV)	Q_β (MeV)
This experiment	-52.89 ± 0.10	8.51 ± 0.10
Myers [a]	−52.61	8.79(8.44)
GHT [b]	−53.80	7.60(7.77)
SH [c]	−52.2	9.2 (9.1)
LZ [d]	−53.37	8.03(8.28)
JGK [e]	−53.01	8.39(8.49)
CK [f]	−53.27	8.13(8.30)

[a] W. D. Myers, Ref. 15.
[b] H. V. Groote, E. R. Hilf, and K. Takahashi, Ref. 15.
[c] P. A. Seeger and W. M. Howard, Ref. 15.
[d] S. Liran and N. Zeldes, Ref. 15.
[e] J. Jänecke, Ref. 15.
[f] E. Comay and I. Kelson, Ref. 15.

B. Ground-state spin and parity of ^{60}Mn

A single-particle shell model predicts that the ground-state configuration of $^{60}_{25}\mathrm{Mn}_{35}$ should be $\pi(1f_{7/2})^{-3}\nu(1f_{5/2})^3$. The ground-state spins and parities of the odd-A Mn isotopes indicate that the $\pi(f_{7/2})^{-3}$ configuration is coupled to $\frac{5}{2}^-$ and that of the adjacent odd-A $N=35$ isotone, ^{61}Fe, indicates that the $\nu(f_{5/2})^3$ configuration can be coupled to $\frac{3}{2}^-$ (Ref. 16). If one assumes the same couplings to be present in ^{60}Mn, then Nordheim's rules, as modified by Brennan and Bernstein,[17] suggest a ground-state spin and parity of 3^+ for ^{60}Mn. It should be noted that ^{54}Mn, ^{56}Mn, and probably ^{58}Mn all have spins and parities of 3^+ (Ref. 16). By analogy, it could be expected that the spin and parity of ^{60}Mn would also be 3^+. However, it should also be pointed out that although the above-mentioned rules predict the correct spins and parities for ^{54}Mn and ^{60}Mn, they fail to predict the correct values for ^{56}Mn and ^{58}Mn.

C. Level structure and electromagnetic transitions in ^{60}Fe

A shell-model calculation of the ^{60}Fe level scheme and electromagnetic transition branching ratios was performed several years ago by Larson, Raman, and McGrory.[18] In this calculation, an inert ^{48}Ca core was assumed. The protons were restricted to the $1f_{7/2}$ shell, and the neutrons were allowed to occupy any vacant $1f$-$2p$ orbital.

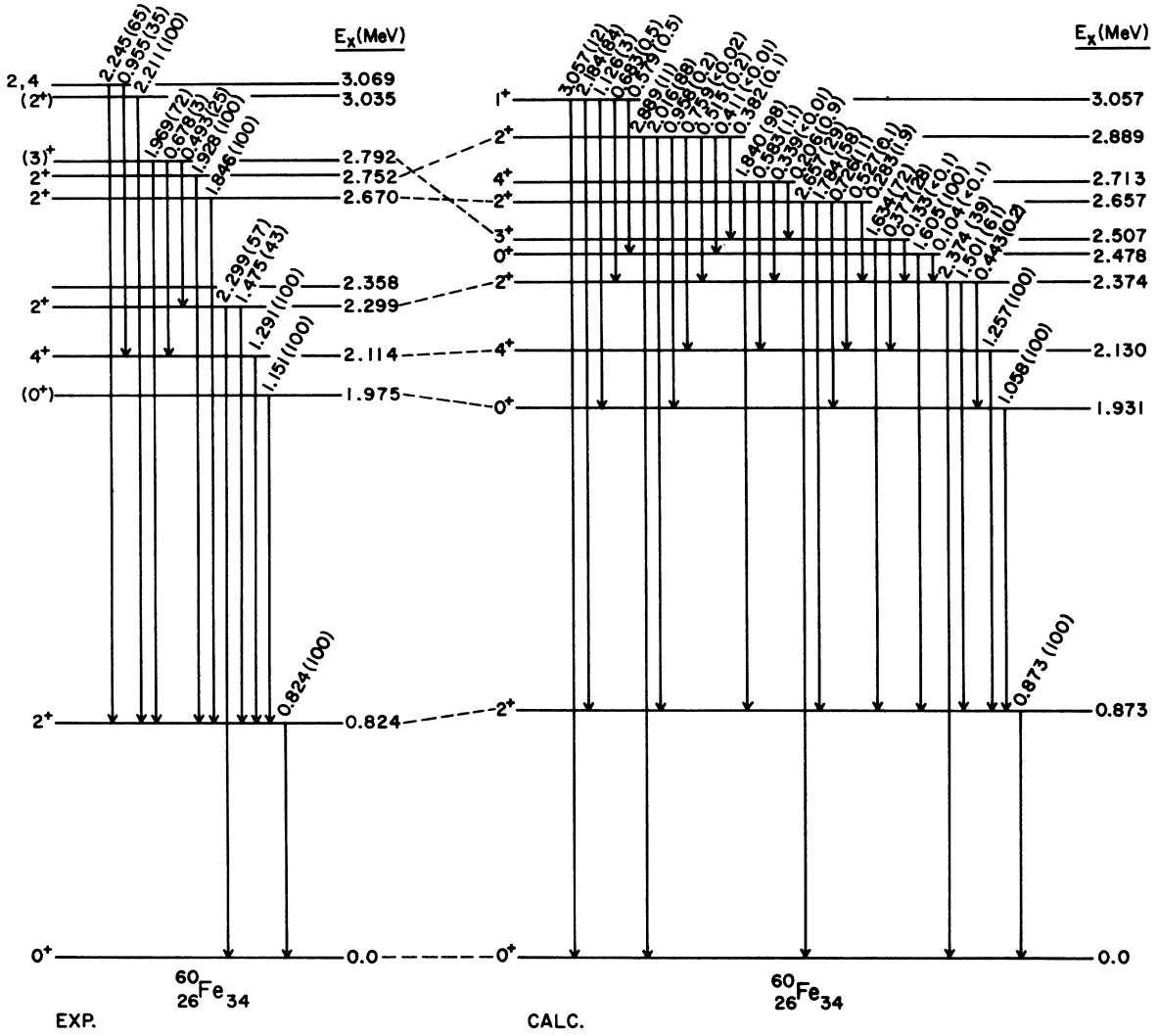

FIG. 7. A comparison of the experimental level structure and electromagnetic transitions below 3.1 MeV in ^{60}Fe with the shell-model calculations of Larson, Raman, and McGrory (Ref. 18). Dashed lines indicate probable correspondences. The experimental level scheme is a compilation of the results of the present work and those of previous studies (Refs. 7 and 8) of ^{60}Fe. The numbers enclosed by parentheses are the branching percentages for each transition.

The form of the interactions and the matrix elements used in this calculation are described by McGrory[19] in his previous studies of ^{56}Cr and ^{58}Fe. Figure 7 shows a comparison of the calculated level structure and electromagnetic transitions in ^{60}Fe with the structure as determined by the present and previous experiments.[7,8]

For excitation energies below 2.4 MeV, the agreement between the calculated and the observed positions of the energy levels is very good. The calculated energies of the first four excited states are all within 75 keV of the observed values, and the predicted ordering of the $0^+, 4^+, 2^+$ triplet is in agreement with experiment. As expected, the 0^+ and 4^+ members of this triplet decay only to the first excited state. The 2^+ member, however, is predicted, and is observed to decay strongly to both the ground state and first excited state. The spin, parity, and decay modes of the observed 2.358-MeV level have not been experimentally determined. As a result, no correspondence has been made between this level and any of the calculated levels.

Above 2.4-MeV excitation energy, there is still reasonable agreement between the calculated and observed level structures. However, the predicted ordering of levels is not in complete agreement with experiment, and some of the calculated levels

have not been observed experimentally. The observed $(3)^+$ level at 2.792-MeV probably corresponds to the calculated 2.507-MeV state. As predicted, its predominant decay mode is to the first 2^+ excited state. The observed branching ratios for the decays to the second 2^+ state and to the first 4^+ state, however, appear to be interchanged with respect to the calculations. Above 2.8-MeV excitation, no correspondences have been made between the observed and the calculated levels.

ACKNOWLEDGMENTS

The authors wish to thank D. Larson, S. Raman, and J. B. McGrory for allowing us to use the results of their shell-model calculations prior to their publication. We also wish to thank D. F. Geesaman, J. P. Schiffer, and S. Raman for careful readings of the manuscript. This work was performed under the auspices of the U.S. Department of Energy.

---

*This work is submitted in partial fulfillment of the requirements for the Ph.D. degree at the University of Chicago.

†Thesis student at ANL from the University of Chicago.

‡Present address: Cyclotron Laboratory, Michigan State University, E. Lansing, Michigan 48824.

[1]C. N. Davids, S. L. Tabor, E. B. Norman, R. C. Pardo, and L. A. Parks, Phys. Rev. C 14, 1601 (1976).

[2]L. A. Parks, C. N. Davids, and R. C. Pardo, Phys. Rev. C 15, 730 (1977).

[3]C. N. Davids, D. F. Geesaman, S. L. Tabor, M. J. Murphy, E. B. Norman, and R. C. Pardo, Phys. Rev. C (to be published).

[4]R. C. Pardo, C. N. Davids, M. J. Murphy, E. B. Norman, and L. A. Parks, Phys. Rev. C 16, 370 (1977).

[5]E. B. Norman, C. N. Davids, M. J. Murphy, R. C. Pardo, and L. A. Parks, Bull. Am. Phys. Soc. 21, 967 (1976).

[6]M. Sakai, in *Proceedings of the Symposium on In-Beam Spectroscopy with Heavy Ions*, edited by H. Kamitsubo (Wako-shi, Saitama, Japan, 1972), p. 114.

[7]E. K. Warburton, J. W. Olness, A. M. Nathan, J. J. Kolata, and J. B. McGrory, Phys. Rev. C 16, 1027 (1977).

[8]E. B. Norman, C. N. Davids, and C. E. Moss, Phys. Rev. C (to be published).

[9]M. Blann, Univ. of Rochester, Nuclear Structure Laboratory, Report No. COO-3494-29 (unpublished).

[10]L. A. Parks, C. N. Davids, B. G. Nardi, and J. N. Worthington, Nucl. Instrum. Methods 143, 93 (1977).

[11]N. B. Gove and M. J. Martin, Nucl. Data A10, 205 (1971).

[12]C. N. Davids, D. R. Goosman, D. E. Alburger, A. Gallman, G. Guillaume, D. H. Wilkinson, and W. A. Lanford, Phys. Rev. C 9, 216 (1974).

[13]S. Raman and N. B. Gove, Phys. Rev. C 7, 1995 (1973).

[14]K. G. Tirsell, L. G. Multhauf, and S. Raman, Phys. Rev. C 10, 785 (1974).

[15]S. Maripuu, At. Data Nucl. Data Tables 17, 489 (1976), 1975 Mass Excess Predictions.

[16]F. W Walker, G. J. Kirouac, and F. M. Rourke, *Chart of the Nuclides* (General Electric Co., Schenectady, New York, 1977), 12th edition.

[17]M. H. Brennan and A. M. Bernstein, Phys. Rev. 120, 927 (1960).

[18]D. Larson, S. Raman, and J. B. McGrory (private communication).

[19]J. B. McGrory, Phys. Lett. 26B, 604 (1968).